# Are Multiphase Competition and Order by Disorder the Keys to Understanding Yb$_2$Ti$_2$O$_7$?

L. D. C. Jaubert,[1] Owen Benton,[1] Jeffrey G. Rau,[2] J. Oitmaa,[3] R. R. P. Singh,[4] Nic Shannon,[1] and Michel J. P. Gingras[2,5,6]

[1]*Okinawa Institute of Science and Technology Graduate University, Onna-son, Okinawa 904-0495, Japan*
[2]*Department of Physics and Astronomy, University of Waterloo, 200 University Avenue West,
Waterloo, Ontario N2L 3G1, Canada*
[3]*School of Physics, The University of New South Wales, Sydney 2052, Australia*
[4]*Department of Physics, University of California, Davis, California 95616, USA*
[5]*Perimeter Institute for Theoretical Physics, 31 Caroline North, Waterloo, Ontario N2L 2Y5, Canada*
[6]*Canadian Institute for Advanced Research, Toronto, Ontario M5G 1Z8, Canada*

If magnetic frustration is most commonly known for undermining long-range order, as famously illustrated by spin liquids, the ability of matter to develop new collective mechanisms in order to fight frustration is perhaps no less fascinating, providing an avenue for the exploration and discovery of unconventional behaviors. Here, we study a realistic minimal model where a number of such mechanisms converge, which, incidentally, pertain to the perplexing quantum spin ice candidate Yb$_2$Ti$_2$O$_7$. Specifically, we explain how thermal and quantum fluctuations, optimized by order-by-disorder selection, conspire to expand the stability region of a degenerate continuous U(1) manifold against the classical splayed ferromagnetic ground state that is displayed by the sister compound Yb$_2$Sn$_2$O$_7$. The resulting competition gives rise to multiple phase transitions, in striking similitude with recent experiments on Yb$_2$Ti$_2$O$_7$ [Lhotel *et al.*, Phys. Rev. B **89**, 224419 (2014)]. By combining a gamut of numerical techniques, we obtain compelling evidence that such multiphase competition is a natural engine for the substantial sample-to-sample variability observed in Yb$_2$Ti$_2$O$_7$ and is the missing key to ultimately understand the intrinsic properties of this material. As a corollary, our work offers a pertinent illustration of the influence of chemical pressure in rare-earth pyrochlores.

The vast interest in magnetic frustration largely stems from the diversity of unconventional phenomena it begets, ranging from the anomalous Hall effect [1] to multiferroicity [2], to name only a few. The reason for this diversity is the indecisiveness of frustrated magnets towards ordering, which opens an avenue for exotic mechanisms to control their low-temperature properties.

This diversity of ordering processes is vividly illustrated within the family of rare-earth pyrochlore compounds [3–7]. In Er$_2$Ti$_2$O$_7$ [8–12], soft modes of excitations are claimed to lift a ground-state degeneracy whose symmetry is U(1), i.e., generated by a continuous rotation of all spins. This order-by-disorder (ObD) mechanism [13] selects the so-called $\psi_2$ over the $\psi_3$ configurations depicted in Figs. 1(b) and 1(c). Recently, Yb$_2$Ti$_2$O$_7$ has also drawn noticeable attention in the context of quantum and thermal spin liquids [6,14,15], the Higgs mechanism [16], ferromagnetic order [14,16–18], and magnetic monopoles [19,20]. Its ordering—or absence of ordering—has been a matter of heated debate for nearly 15 years [16–18, 21–25], complicated by sample-dependence issues [24,26,27], which suggest the influence of structural disorder as in Tb$_2$Ti$_2$O$_7$ [28] or Dy$_2$Ti$_2$O$_7$ [29].

Under such circumstances, we believe that in order to make progress in understanding Yb$_2$Ti$_2$O$_7$ it is necessary to search for unifying patterns. Recent bulk measurements [18] are particularly enlightening in that respect, as they provide compelling evidence for multistep ordering in putative disorder-free Yb$_2$Ti$_2$O$_7$, common to both powder and single crystals. Our motivation here is twofold. First, we present a thorough analysis of multiphase competition for a range of parameters near those found to describe Yb$_2$Ti$_2$O$_7$ [14]. We show how both thermal and quantum fluctuations enhance the stability of the degenerate U(1) manifold previously observed in Er$_2$Ti$_2$O$_7$, to the detriment of a splayed ferromagnetic (SFM) phase displayed in Fig. 1(d). Then, we apply our theory to Yb$_2$Ti$_2$O$_7$, successfully accounting for the unusual multistep ordering process and field dependence observed in Ref. [18]. By explaining the nature of this competition, our theory provides a natural setting to rationalize the sample dependence of Yb$_2$Ti$_2$O$_7$ [26,33] and the influence of chemical pressure in Yb-based pyrochlores [34].

*Model.*—The crystal electric field of Yb$^{3+}$ ions in Yb$_2$Ti$_2$O$_7$ has a Kramers ground doublet, well isolated by 600 K from the excited doublets [35], giving rise to a pseudospin-1/2 degree of freedom $\vec{S}$. The resulting effective Hamiltonian can be described by four independent nearest-neighbor anisotropic couplings $\{J_{i=1..4}\}$ respecting the symmetries of the pyrochlore lattice [4,36]:
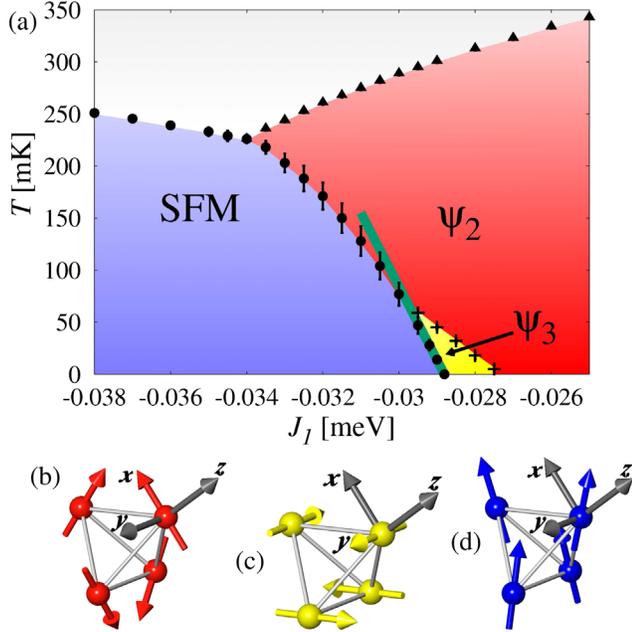
FIG. 1 (color online). (a) Multiphase competition of the anisotropic nearest-neighbor pyrochlore model of Eq. (1), as determined by classical Monte Carlo simulations for $\{J_{i=2,3,4}\} = \{-0.22, -0.29, 0\}$ meV [30]. The $\psi_2$ and $\psi_3$ phases are selected by order by disorder within the antiferromagnetic U(1) manifold and separated from the splayed ferromagnet (SFM) by a first-order transition, whose slope agrees with classical low-temperature expansion (green line) [30,31]. The local $(x, y, z)$ axes are, respectively, defined along the local $\langle \bar{1}\bar{1}2\rangle$, $\langle 1\bar{1}0\rangle$, and $\langle 111\rangle$ directions. The spins of the $\psi_2$ (b) and $\psi_3$ (c) states point along their local $x$ and $y$ axes, respectively [32]. Rotating all spins of a given $\psi_2$ state by the same angle about their local $z$ axis generates the entire U(1) manifold, including the $\psi_3$ states. The spins of the SFM states (d) are canted away from a global cubic axis by the same angle towards their local $z$ axis. Each of the SFM, $\psi_2$, and $\psi_3$ phases are sixfold degenerate.

$$\mathcal{H} = \sum_{\langle ij \rangle} \vec{S}_i \bar{\mathcal{J}}_{ij} \vec{S}_j \quad \text{with} \quad \bar{\mathcal{J}} = \begin{pmatrix} J_2 & J_4 & J_4 \\ -J_4 & J_1 & J_3 \\ -J_4 & J_3 & J_1 \end{pmatrix}. \quad (1)$$

All coupling matrices $\bar{\mathcal{J}}_{ij}$ can be deduced from $\bar{\mathcal{J}}$ by appropriate symmetry transformations [14]. Our work focuses on the parameter line $J_1 \in [-0.09 : 0]$ meV and $\{J_{i=2,3,4}\} = \{-0.22, -0.29, 0\}$ meV, relevant to $Yb_2Ti_2O_7$ for $J_1 = -0.09(3)$ [37] [14] and including the $T = 0$ boundary between the SFM and U(1) phases at $J_1 = -0.029$ [see Fig. 1(a)]. We consider both quantum $S = 1/2$ and classical O(3) spins ($|\vec{S}| = 1/2$) whose phase diagrams can be found in Refs. [6,7,11,15,38,39].

*Classical thermal fluctuations.*—The classical ground states of Eq. (1) are described in Figs. 1(b)–1(d) and have been identified in Refs. [4,7]. At $T = 0$, the SFM order persists for $J_1 < -0.029$ before giving way to the one-dimensional U(1) manifold for $J_1 > -0.029$. At the boundary,

new continuously degenerate ground states emerge, which confer additional zero-mode fluctuations to $\psi_3$ states [7].

This zero-temperature framework sets the scene for the phase diagram of Fig. 1(a) computed by Monte Carlo (MC) simulations [30,40–42]. The U(1) degeneracy does not survive thermal fluctuations, collapsing predominantly in the $\psi_2$ configurations, except for a small $\psi_3$ island around the boundary due to the aforementioned soft modes of excitations. The selection of the $\psi_2$ and $\psi_3$ phases optimizes the entropy of the U(1) manifold for a given set of parameters and temperature. At finite temperature, this optimization puts the energetically selected SFM phase at a disadvantage and gives rise to multiple phase transitions for $J_1 \in [-0.034 : -0.029]$. Since the Hamiltonian of Eq. (1) supports a large variety of emergent degeneracies and potential ObD transitions at the boundaries between ordered phases [7,43], we expect such a phenomenology to be a common feature of pyrochlores [44–46] and frustrated magnetism [47]. But since temperature is not the only source of fluctuations, how do quantum fluctuations fit in this picture?

*Quantum fluctuations at zero temperature.*—Knowing the competing SFM, $\psi_2$, and $\psi_3$ classical phases, one may analyze their stability in the semiclassical limit using linear spin-wave theory (LSW) [48]. While nonlinear spin wave theory is usually necessary when expanding around classically unstable states, linear calculations become tractable when adding a positive-definite term to the semiclassical energy of the unstable states [30,49]. Doing so gives an upper bound of the semiclassical $\psi_2$ and $\psi_3$ energies for $J_1 < -0.029$ meV. Keeping in mind that this approach underestimates the stability of the U(1) manifold, LSW shows that the semiclassical $T = 0$ frontier is shifted by quantum zero-point fluctuations from $-0.029$ down to $-0.062$ meV (see Table I).

We now consider quantum spins $1/2$. Since frustration is already at play in the constituting bricks of the pyrochlore lattice, namely the tetrahedra, exact diagonalization (ED) of a finite number of tetrahedra provides a good indication of the local influence of quantum effects. To preserve the symmetry of the pyrochlore lattice, we consider clusters of

TABLE I.  Critical value of the exchange parameter $J_1$ in meV, separating the SFM from the U(1) manifold, as estimated from MC simulations, linear spin-wave theory (LSW), exact diagonalization (ED), numerical linked-cluster computation (NLC), and high-temperature expansion (HTE), at zero temperature and upon cooling from high temperature. Quantum and thermal fluctuations jointly stabilize the U(1) manifold over the SFM phase and bring the SFM and U(1) boundary within the error bars of the $Yb_2Ti_2O_7$ parameters [14].

| | Classical | | Quantum | | |
| | MC | LSW | ED | NLC | HTE |
|---|---|---|---|---|---|
| $T > 0$ | $-0.0340(5)$ | $\cdots$ | $\cdots$ | $-0.070(3)$ | $-0.06(3)$ |
| $T = 0$ | $-0.0289(1)$ | $-0.062$ | $-0.064(2)$ | $\cdots$ | $\cdots$ |

4 and 16 spins, forming respectively one and five tetrahedra and allowing for standard ED. Defining the order parameter $M$ and associated correlator $C = \langle M^2 \rangle - \langle M \rangle^2$ of a given phase, the quantity $\Delta C = C_{U(1)} - C_{SFM}$ is then a direct measure of the SFM and U(1) competition, bringing the $T = 0$ frontier to $J_1 \approx -0.052(2)$ and $-0.064(2)$ for $N = 4$ and $N = 16$, respectively [30], in agreement with the semiclassical results (see Table I).

*Quantum fluctuations at finite temperature.*—Even if the combined analysis of thermal and quantum fluctuations is challenging for such a frustrated problem, the buildup of correlations upon approaching the transitions from high temperature remains accessible thanks to numerical linked-cluster computation (NLC) [30,50–52] and high-temperature series expansion (HTE) [12,30,53].

HTE confirms the shifting of the boundary down to $J_1 = -0.06(3)$ meV and with transition temperatures lower than 500 mK (see the inset of Fig. 2). As for NLC, at high temperature where quantum effects ultimately disappear, $\Delta C$ changes sign at the classical limit $J_1 \approx -0.03$ meV, which can be understood from the $\beta^2$ terms in HTE. Then, as temperature decreases for $J_1 < -0.03$, instead of diverging towards SFM ordering, $\Delta C$ shows a clear upturn towards enhanced U(1) correlations (see Fig. 2). This upturn is adiabatically evolving to lower temperature as $J_1$ is decreased, putting the U(1) and SFM frontier at $J_1 = -0.070(3)$ meV.

In summary, although each method used here is subject to its own limitations, they give in concert a highly consistent picture: the classical phase diagram of Fig. 1(a) is shifted by quantum fluctuations. This quantum shifting is already present at the semiclassical level and for temperatures noticeably higher than the classical transition
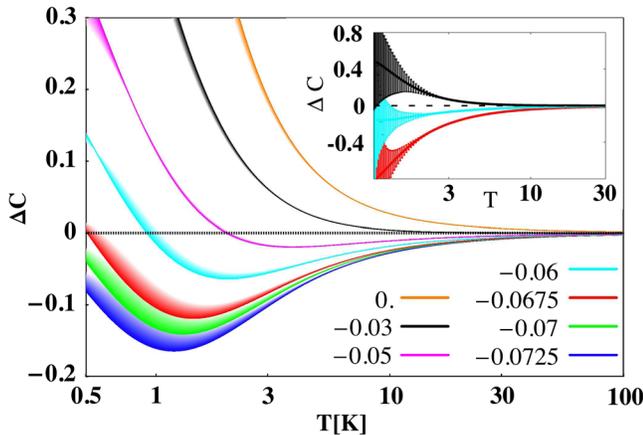


FIG. 2 (color online). The difference in the correlators $\Delta C = C_{U(1)} - C_{SFM}$ computed with NLC confirms the quantum shifting of the boundary towards more negative values of $J_1$ than for the classical system, estimated at $J_1 = -0.070(3)$ meV. $J_1$ is given in the caption while $\{J_{i=2,3,4}\} = \{-0.22, -0.29, 0\}$. Inset: $\Delta C$ as computed from HTE for $J_1 = -0.09$ (red), $-0.06$ (cyan), and $-0.03$ (black). The breadth of each curve represents the uncertainty for NLC and HTE at low temperature.

temperatures. Our results, summarized in Table I, suggest the same qualitative shape of the U(1) and SFM boundary for quantum spins $S = 1/2$ as for classical ones.

*Multiphase competition in* $Yb_2Ti_2O_7$.—While the parametrization of $Yb_2Ti_2O_7$ used here $\{J_{i=1,2,3,4}\} = \{-0.09(3), -0.22(3), -0.29(2), 0.01(2)\}$ meV, obtained by inelastic neutron scattering under a large field [14], has been useful to understand the paramagnetic and high field regimes [7,14–16,51,54], many questions remain open at low temperature and a zero field.

Based on the experiments of Ref. [18], and thanks to the present analysis, we believe it is possible to flesh out a common framework for the powder and single crystal samples that do display magnetic order. Upon cooling, both samples undergo (i) a nonferromagnetic transition signaled by a peak in the specific heat, followed by (ii) a first-order ferromagnetic transition observed in superconducting quantum interference device (SQUID) measurements. The transition temperatures are 150 and 195 mK for the single crystal, and 245 and 265 mK for the powder sample. Furthermore, the application of a magnetic field $h$ does not destroy the low-temperature ferromagnetic transition, but rather increases its temperature for $h > 5$ mT. The transition remains first order up to $h_c \approx 20$ mT, before becoming continuous or vanishing, which is experimentally difficult to distinguish. These experimental results fit perfectly with our theory. The double transition is a direct consequence of the SFM and U(1) competition, as shown in Fig. 1(a) and for a similar range of temperatures as in experiments. Furthermore, since the U(1) manifold is antiferromagnetic, it does not couple with $h$. The magnetic field thus only favors the SFM phase, and the first-order ferromagnetic transition is expected to persist until the U(1) phase is destroyed at $h_c$. MC simulations confirm this scenario with $h_c \approx 15$ mT, followed by a crossover for $h > h_c$ [see Fig. 3(b)]. Interestingly, the single crystal magnetization also displays a reversible bump at $\approx 180$ mK between the two transitions. According to our MC simulations, such a feature could correspond to a $\psi_2$ to $\psi_3$ ObD transition, but with the caveat that the $\psi_3$ phase does not persist above 50 mK in our classical phase diagram. In that case, structural disorder may play an important role [28,29,33], since it is known (i) to favor $\psi_3$ over $\psi_2$ order [55] and (ii) to be stronger in single crystals than in powder samples where no bump is observed [18].

It should be noted that our results leave open the possibility for a thermal spin liquid above the transition temperatures [15]. Also, even if the parametrization that we used, taken from Ref. [14], was done on samples different from the ones in Ref. [18], the quantum shifting of the SFM and U(1) boundary brings this classical scenario within the experimental uncertainty of the $J_1 = -0.09 \pm 0.03$ meV parametrization range. This quantum shifting is best illustrated in Fig. 3(a), where the structure factor calculated from classical simulations at $J_1 = -0.0335$ meV is almost identical to quantum (NLC) results at $J_1 = -0.06$ meV. As for neutron scattering measurements of $Yb_2Ti_2O_7$ [see Fig. 2(a) of
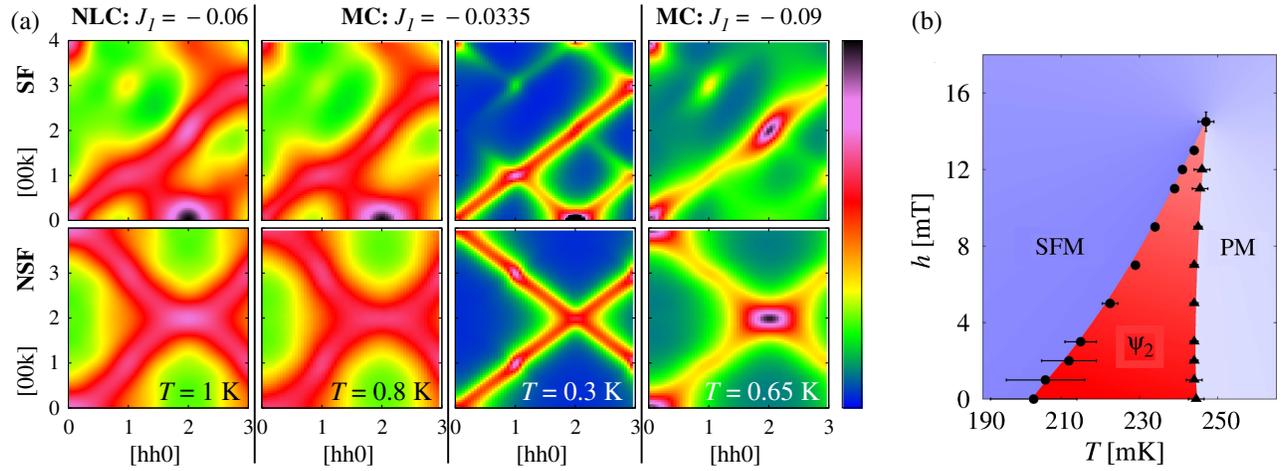
FIG. 3 (color online).    Application to $Yb_2Ti_2O_7$. (a) Structure factor as measured by neutron scattering and (b) phase diagram in a field. (a) The spin flip (SF, top panels) and nonspin flip (NSF, bottom panels) calculated by quantum NLC and classical Monte Carlo simulations are almost identical when $J_1$ is shifted from $-0.0335$ to $-0.06$ meV (please note that the temperature has been renormalized by 5/4 for a better agreement). This agreement confirms the quantum shifting of the boundary at finite temperature. When approaching the phase transition, the MC structure factor for $J_1 = -0.0335$ meV reproduces the characteristic features of $Yb_2Ti_2O_7$ neutron scattering data measured at 300 mK [to be compared with Fig. 2(a) of Ref. [16]]. On the other hand, the agreement between experiments [16] and classical simulations using the parametrization of Ref. [14] ($J_1 = -0.09$ meV) is noticeably less successful, especially around (220) [7]. This disagreement is not a criticism of the parametrization by Ross *et al.*, but rather an emphasis on the importance of quantum fluctuations. The temperature of 0.65 K in the right panels has been chosen such that the ratio between the measurement and transition temperatures is the same as in Ref. [16]. The color scale is fixed from zero to the maximum SF intensity, except for the panel at 0.3 K where the color scale was chosen for visual comparison with experiments [16]. The SF and NSF channels, respectively, consider spin components along the $[1\bar{1}0]$ direction and orthogonal to $[1\bar{1}0]$ and to the wave vector $\vec{q}$ in the [hhk] plane. (b) When a field is applied along the [001] direction, the antiferromagnetic $\psi_2$ phase gradually disappears in the MC simulations. Our theory thus explains why the first-order transition only persists at a low field in $Yb_2Ti_2O_7$ [18]. We used $J_1 = -0.033$ meV and the anisotropic $g$ tensor of $Yb_2Ti_2O_7$ [35]: $g_\perp = 4.18$ and $g_\perp = 1.77$.

Ref. [16]], the agreement is noticeably better with classical simulations for $J_1 = -0.0335$ meV where a double transition takes place than for $J_1 = -0.09$ meV, confirming once more the relevance of our theory to $Yb_2Ti_2O_7$.

Last but not least, our work brings $Yb_2Ti_2O_7$ as the missing link between $Yb_2Sn_2O_7$ and $Yb_2Ge_2O_7$, whose ground states are respectively splayed ferromagnetic [56,57], and a not yet characterized antiferromagnet [34], which we tentatively associate with U(1). On the basis of our theory, we anticipate that a natural path will take this series of compounds through a transition from a SFM phase to a U(1) manifold via chemical pressure (Sn → Ti → Ge), in analogy with spin ice materials [58,59].

*Conclusion.*—Our work sets $Yb_2Ti_2O_7$ as a paragon of the complexity of ordering mechanisms in frustrated magnets. Using a palette of complementary numerical methods, we have shown how the multistep ordering and field dependence observed in certain powder and single crystals [18] naturally arises from the competition between a SFM phase and a U(1) manifold, whose boundary is shifted by quantum fluctuations and mediated by order-by-disorder selection. In the general context of multiphase competition, order by disorder can be viewed as a free-energy optimization process that reinforces the stability of the degenerate phase it acts upon by selecting the subset of configurations with higher entropy and/or quantum zero-point fluctuations.

In light of the numerous models and phases supported by pyrochlores, ranging from spin liquids and spin ices to (partially) ordered phases [3,6,15,60–63], and subsequent boundaries between them [7,45,46], our present work is a paradigmatic example of why the properties of frustrated magnets should generically be understood as the convergence of competing phases, rather than originating from a single controlling state. Experimentally, some of these properties would indeed seem to be "coming from nowhere" in the absence of a global phase diagram. We expect such a competition between neighboring phases to be particularly relevant to some of the most difficult materials to characterize, such as $Tb_2Ti_2O_7$ [28] and $Er_2Sn_2O_7$ [7,64,65], and to exacerbate the sample dependence issues [28,29,33] by the proximity of phase boundaries. In that respect it is interesting to note that $Er_2Ti_2O_7$, whose coupling parameters lie far away from any phase boundary [7,9,11], is one of the most robust rare-earth pyrochlores for reproducibility of experiments, while $Yb_2Ti_2O_7$ is essentially the antithesis. Hence, we expect the interplay between multiphase competition and disorder to become a very topical question, necessary to account for experiments in pyrochlores and frustrated magnetism, and promisingly rich in exotic physics.

*Note added.*—A paper–now published in Ref. [66]–appeared on arXiv shortly after ours, whose results are consistent with our theory when there is overlap. Also, our prediction of the U(1) nature of the $Yb_2Ge_2O_7$ ground state has now been experimentally confirmed in Ref. [67].

[1] Y. Taguchi, Y. Oohara, H. Yoshizawa, N. Nagaosa, and Y. Tokura, Science **291**, 2573 (2001).

[2] M. Mostovoy, Phys. Rev. Lett. **96**, 067601 (2006).

[3] J. S. Gardner, M. J. P. Gingras, and J. E. Greedan, Rev. Mod. Phys. **82**, 53 (2010).

[4] S. H. Curnoe, Phys. Rev. B **75**, 212404 (2007).

[5] P. A. McClarty, S. H. Curnoe, and M. J. P. Gingras, J. Phys. Conf. Ser. **145**, 012032 (2009).

[6] L. Savary and L. Balents, Phys. Rev. Lett. **108**, 037202 (2012).

[7] H. Yan, O. Benton, L. D. C. Jaubert, and N. Shannon, arXiv:1311.3501.

[8] J. D. M. Champion and P. C. W. Holdsworth, J. Phys. Condens. Matter **16**, S665 (2004).

[9] L. Savary, K. A. Ross, B. D. Gaulin, J. P. C. Ruff, and L. Balents, Phys. Rev. Lett. **109**, 167201 (2012).

[10] M. E. Zhitomirsky, M. V. Gvozdikova, P. C. W. Holdsworth, and R. Moessner, Phys. Rev. Lett. **109**, 077204 (2012).

[11] A. W. C. Wong, Z. Hao, and M. J. P. Gingras, Phys. Rev. B **88**, 144402 (2013).

[12] J. Oitmaa, R. R. P. Singh, B. Javanparast, A. G. R. Day, B. V. Bagheri, and M. J. P. Gingras, Phys. Rev. B **88**, 220404 (2013).

[13] J. Villain, R. Bidaux, J. P. Carton, and R. Conte, J. Phys. (Paris) **41**, 1263 (1980).

[14] K. A. Ross, L. Savary, B. D. Gaulin, and L. Balents, Phys. Rev. X **1**, 021002 (2011).

[15] L. Savary and L. Balents, Phys. Rev. B **87**, 205130 (2013).

[16] L.-J. Chang, S. Onoda, Y. Su, Y.-J. Kao, K.-D. Tsuei, Y. Yasui, K. Kakurai, and M. R. Lees, Nat. Commun. **3**, 992 (2012).

[17] Y. Yasui, M. Soda, S. Iikubo, M. Ito, M. Sato, N. Hamaguchi, T. Matsushita, N. Wada, T. Takeuchi, N. Aso, and K. Kakurai, J. Phys. Soc. Jpn. **72**, 3014 (2003).

[18] E. Lhotel, S. R. Giblin, M. R. Lees, G. Balakrishnan, L. J. Chang, and Y. Yasui, Phys. Rev. B **89**, 224419 (2014).

[19] L. Pan, S. K. Kim, A. Ghosh, C. M. Morris, K. A. Ross, E. Kermarrec, B. D. Gaulin, S. M. Koohpayeh, O. Tchernyshyov, and N. P. Armitage, Nat. Commun. **5**, 4970 (2014).

[20] L. Pan, N. J. Laurita, K. A. Ross, E. Kermarrec, B. D. Gaulin, and N. P. Armitage, arXiv:1501.05638.

[21] J. A. Hodges, P. Bonville, A. Forget, A. Yaouanc, P. Dalmas de Réotier, G. André, M. Rams, K. Królas, C. Ritter, P. C. M. Gubbens, C. T. Kaiser, P. J. C. King, and C. Baines, Phys. Rev. Lett. **88**, 077204 (2002).

[22] J. S. Gardner, G. Ehlers, N. Rosov, R. W. Erwin, and C. Petrovic, Phys. Rev. B **70**, 180404 (2004).

[23] K. A. Ross, J. P. C. Ruff, C. P. Adams, J. S. Gardner, H. A. Dabkowska, Y. Qiu, J. R. D. Copley, and B. D. Gaulin, Phys. Rev. Lett. **103**, 227202 (2009).

[24] R. M. D'Ortenzio, H. A. Dabkowska, S. R. Dunsiger, B. D. Gaulin, M. J. P. Gingras, T. Goko, J. B. Kycia, L. Liu, T. Medina, T. J. Munsie, D. Pomaranski, K. A. Ross, Y. J. Uemura, T. J. Williams, and G. M. Luke, Phys. Rev. B **88**, 134428 (2013).

[25] L.-J. Chang, M. R. Lees, I. Watanabe, A. D. Hillier, Y. Yasui, and S. Onoda, Phys. Rev. B **89**, 184416 (2014).

[26] A. Yaouanc, P. Dalmas de Réotier, C. Marin, and V. Glazkov, Phys. Rev. B **84**, 172408 (2011).

[27] K. A. Ross, L. R. Yaraskavitch, M. Laver, J. S. Gardner, J. A. Quilliam, S. Meng, J. B. Kycia, D. K. Singh, T. Proffen, H. A. Dabkowska, and B. D. Gaulin, Phys. Rev. B **84**, 174442 (2011).

[28] T. Taniguchi, H. Kadowaki, H. Takatsu, B. Fåk, J. Ollivier, T. Yamazaki, T. J. Sato, H. Yoshizawa, Y. Shimura, T. Sakakibara, T. Hong, K. Goto, L. R. Yaraskavitch, and J. B. Kycia, Phys. Rev. B **87**, 060408 (2013).

[29] G. Sala, M. J. Gutmann, D. Prabhakaran, D. Pomaranski, C. Mitchelitis, J. B. Kycia, D. G. Porter, C. Castelnovo, and J. P. Goff, Nat. Mater. **13**, 488 (2014).

[30] See Supplemental Material at http://link.aps.org/supplemental/10.1103/PhysRevLett.115.267208 for a definition of the order parameters of the SFM and U(1) phases and technical details on the methods used in this Letter.

[31] N. Shannon, K. Penc, and Y. Motome, Phys. Rev. B **81**, 184409 (2010).

[32] A. Poole, A. S. Wills, and E. Lelievre-Berna, J. Phys. Condens. Matter **19**, 452201 (2007).

[33] K. A. Ross, T. Proffen, H. A. Dabkowska, J. A. Quilliam, L. R. Yaraskavitch, J. B. Kycia, and B. D. Gaulin, Phys. Rev. B **86**, 174424 (2012).

[34] Z. L. Dun, M. Lee, E. S. Choi, A. M. Hallas, C. R. Wiebe, J. S. Gardner, E. Arrighi, R. S. Freitas, A. M. Arevalo-Lopez, J. P. Attfield, H. D. Zhou, and J. G. Cheng, Phys. Rev. B **89**, 064401 (2014).

[35] J. A. Hodges, P. Bonville, A. Forget, M. Rams, K. Krolas, and G. Dhalenne, J. Phys. Condens. Matter **13**, 9301 (2001).

[36] S. H. Curnoe, Phys. Rev. B **78**, 094418 (2008).

[37] The number between parentheses represents the error bar on the last digit, i.e., $J_1 = -0.09 \pm 0.03$ meV here.

[38] S. B. Lee, S. Onoda, and L. Balents, Phys. Rev. B **86**, 104412 (2012).

[39] Z. Hao, A. G. R. Day, and M. J. P. Gingras, Phys. Rev. B **90**, 214430 (2014).

[40] R. H. Swendsen and J.-S. Wang, Phys. Rev. Lett. **57**, 2607 (1986).

[41] C. J. Geyer, in *Computing Science and Statistics: Proceedings of the 23rd Symposium on the Interface, Seattle, Washington, 1991* (Interface Foundation of North America, Fairfax Station, VA, 1991), p. 156.

[42] M. Creutz, Phys. Rev. D **36**, 515 (1987).

[43] O. Benton, Ph.D. thesis, University of Bristol, 2014.

[44] B. Canals, M. Elhajal, and C. Lacroix, Phys. Rev. B **78**, 214431 (2008).

[45] G.-W. Chern, arXiv:1008.3038.

[46] P. A. McClarty, P. Stasiak, and M. J. P. Gingras, Phys. Rev. B **89**, 024425 (2014).

[47] C. Pinettes, B. Canals, and C. Lacroix, Phys. Rev. B **66**, 024422 (2002).

[48] P. Fazekas, *Lecture Notes on Electron Correlation and Magnetism* (World Scientific, Singapore, 1999).

[49] T. Coletta, M. E. Zhitomirsky, and F. Mila, Phys. Rev. B **87**, 060407 (2013).

[50] M. Rigol, T. Bryant, and R. R. P. Singh, Phys. Rev. E **75**, 061118 (2007).

[51] R. Applegate, N. R. Hayre, R. R. P. Singh, T. Lin, A. G. R. Day, and M. J. P. Gingras, Phys. Rev. Lett. **109**, 097205 (2012).

[52] B. Tang, E. Khatami, and M. Rigol, Comput. Phys. Commun. **184**, 557 (2013).

[53] J. Oitmaa, C. Hamer, and W. Zheng, *Series Expansion Methods for Strongly Interacting Lattice Models* (Cambridge University Press, Cambridge, England, 2006).

[54] N. R. Hayre, K. A. Ross, R. Applegate, T. Lin, R. R. P. Singh, B. D. Gaulin, and M. J. P. Gingras, Phys. Rev. B **87**, 184423 (2013).

[55] V. S. Maryasin and M. E. Zhitomirsky, Phys. Rev. B **90**, 094412 (2014).

[56] A. Yaouanc, P. Dalmas de Réotier, P. Bonville, J. A. Hodges, V. Glazkov, L. Keller, V. Sikolenko, M. Bartkowiak, A. Amato, C. Baines, P. J. C. King, P. C. M. Gubbens, and A. Forget, Phys. Rev. Lett. **110**, 127207 (2013).

[57] Z. L. Dun, E. S. Choi, H. D. Zhou, A. M. Hallas, H. J. Silverstein, Y. Qiu, J. R. D. Copley, J. S. Gardner, and C. R. Wiebe, Phys. Rev. B **87**, 134408 (2013).

[58] H. D. Zhou, J. G. Cheng, A. M. Hallas, C. R. Wiebe, G. Li, L. Balicas, J. S. Zhou, J. B. Goodenough, J. S. Gardner, and E. S. Choi, Phys. Rev. Lett. **108**, 207206 (2012).

[59] C. R. Wiebe and A. M. Hallas, APL Mater. **3**, 041519 (2015).

[60] M. J. P. Gingras and P. A. McClarty, Rep. Prog. Phys. **77**, 056501 (2014).

[61] M. E. Brooks-Bartlett, S. T. Banks, L. D. C. Jaubert, A. Harman-Clarke, and P. C. W. Holdsworth, Phys. Rev. X **4**, 011007 (2014).

[62] B. Javanparast, Z. Hao, M. Enjalran, and M. J. P. Gingras, Phys. Rev. Lett. **114**, 130601 (2015).

[63] J. G. Rau and M. J. P. Gingras, Phys. Rev. B **92**, 144417 (2015).

[64] P. M. Sarte, H. J. Silverstein, B. T. K. V. Wyk, J. S. Gardner, Y. Qiu, H. D. Zhou, and C. R. Wiebe, J. Phys. Condens. Matter **23**, 382201 (2011).

[65] S. Guitteny, S. Petit, E. Lhotel, J. Robert, P. Bonville, A. Forget, and I. Mirebeau, Phys. Rev. B **88**, 134408 (2013).

[66] J. Robert, E. Lhotel, G. Remenyi, S. Sahling, I. Mirebeau, C. Decorse, B. Canals, and S. Petit, Phys. Rev. B **92**, 064425 (2015).

[67] Z. L. Dun, X. Li, R. S. Freitas, E. Arrighi, C. R. Dela Cruz, M. Lee, E. S. Choi, H. B. Cao, H. J. Silverstein, C. R. Wiebe, J. G. Cheng, and H. D. Zhou, Phys. Rev. B **92**, 140407 (2015).